J. Trop. Agric. and Fd. Sc. 43(2)(2015): 191 – 201

Effects of different cross-section shapes on bending and weight of harvesting pole by using finite element analysis

A.R. Rohazrin[1], M.R. Azmin Shakrine[2], Z. Rizal[2] and A. Mohamed Tarmizi[2]

[1]Mechanisation and Automation Research Centre, MARDI Headquarters, Serdang, P.O. Box 12301, 50774 Kuala Lumpur, Malaysia
[2]Faculty of Engineering, Universiti Putra Malaysia, 43400 UPM Serdang, Selangor, Malaysia

Abstract
Harvesting pole is a main requirement in harvesting activity that involves tall trees. A long pole always has problems with bending and weight. Study on the effect of cross-section shapes on bending and weight may give some information about the best design for harvesting pole. Laboratory testing is expensive and time consuming. Finite element analysis using computer software is the best method and cost less. A total of six designs of pole cross-section were tested using Pro-Mechanica software for obtaining their bending/deflection. The six shapes are circular, hexagon, octagon, decagon, icosagon and ellipse. A total of five testings were implemented, that consist of combination of three pole conditions, loaded/unloaded, end/middle constrained and same/different weight. The analyses results show that the circular cross-section shape is the strongest shape to resist bending. Ellipse cross-section shape has different value of bending depends on the orientation. Final evaluation shows circular and icosagon were the best cross-section of harvesting pole.

Keyword: cross-section, harvesting pole, bending

Introduction

Harvesting is a process of collecting mature fruits of crops at field. Harvesting activities for tall trees require a long pole to reach the fruit. Pole can be made of bamboo, wood or metal. In oil palm production industry, pole is a main tool for harvesting process that uses about 60% of the work force and accounts about 50% of the production cost (Malek 1993). Pole is used by lifting and holding it at the required position. Usually, a cutting device is mounted at the tip of the pole. The cutting device can either be a sickle, scissors or saw. The latest invention is a motorised sickle called CANTAS that has been used in the oil palm production industry (Abdul Razak 2008).

In 1988, Palm Oil Research Institute of Malaysia (PORIM) introduced aluminium pole to overcome some of the disadvantages of bamboo. During that time, aluminium pole was not manufactured for harvesting purpose, so a lot of studies had been conducted to improve and obtain the best design. A good harvesting pole should has the following characteristics: good flexibility, lightweight, ergonomic and durable (Abd. Halim 1988). Lightweight poles can increase efficiency of the harvesting process and reduce worker's back strain (Abdul Razak 2002).

Bending and weight have always been the problems in lifting operation of harvesting pole. Bending occurs due to high

Article history
Received: 24.9.2012
Accepted: 6.3.2015

Authors' full names: Rohazrin Abdul Rani, Azmin Shakrine Mohd Rafie, Rizal Zahari and Mohamed Tarmizi Ahmad
E-mail: rohazrin@mardi.gov.my

flexibility and heaviness which is related to size and material. Aluminium alloy 2014 has been introduced as the based material for the current pole because it offers the desired characteristics as proven in the aircraft applications (Abdul Razak 1999). Abd Halim (1988) found that the ellipse cross-section is the best shape to resist deflection. The study was done in laboratory and the study was limited to certain cross section. There are other cross-sections that can be used to enhance the capability of the pole in preventing deflection.

Nowadays, there are many computer applications for solving engineering problem. Finite element analysis (FEA) software is widely used in engineering design activity. The FEA is a problem solving approach for practical (engineering) problems. The problems are first converted into matrix and partial differential equation form. The partial differential and integral equations are solved to obtain the solution of the problem. The number of the equations to be solved is usually large and practically impossible to obtain the solution without using computer. This calls for the need of different FEA packages. There are many FEA packages available for different applications. Some popular FEA packages are Pro-Mechanica, Ansys, Nastran and Gambit etc (Suvo 2010).

The objective of this study was to stimulate the effect of different cross-section shape on pole mechanical properties specific to the bending and weight using FEA to gather information for designing better harvesting pole. The use of FEA is cheaper and faster as compared to laboratory test that involves designing and constructing the pole, which is expensive and time consuming.

Materials and methods

In this study, three applications softwares were used, Pro-Engineer for CAD modeling, Pro-Mechanica for FEAs study and MathCAD as an engineering calculation solver. Pro-Engineer is a 3D CAD based modeling software and Pro-Mechanica is a module within Pro-Engineer that enables users to perform FEA simulations on their product design so that they can pre-determine whether the design fulfil their requirement before fabrication. There are two main Pro-Mechanica modules: structural and thermal. Pro-Mechanica structural analysis enables the users to perform static, modal, buckling, contact, prestress static and et cetera. For this study, only static analysis was used. *Figure 1* is the standard procedure of finite element analysis using Pro-Mechanica.

Harvesting pole is a simple structure, a straight long tube with specific even cross-section along the length. By using Pro-Engineer, the pole was illustrated as a single line with specific length of 9000 mm. The single line was preferred rather than solid because analysis time was short. The pole was constructed as a horizontal line in XY plane in SKETCH environment,

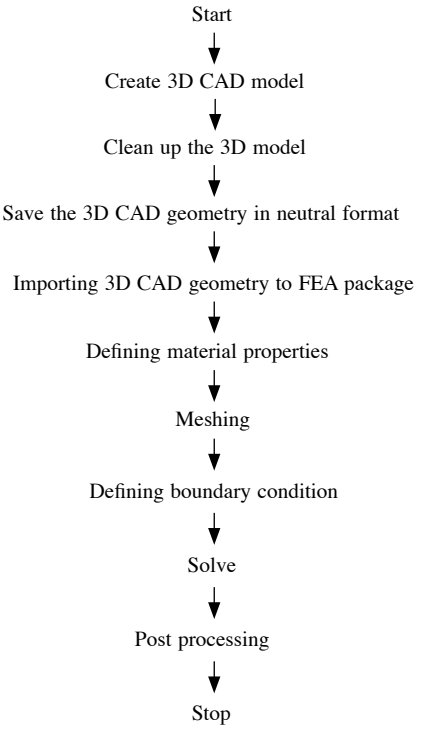

Figure 1. Flow of finite element analysis using Pro-Mechanica

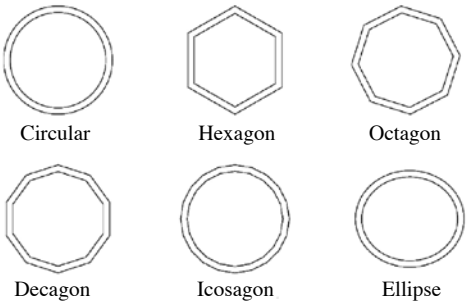

Figure 2. Pole cross-section

meanwhile the cross-sections of the pole were constructed in Pro-Mechanica analysis environment. A total of six cross-sections namely circular, hexagon, octagon, decagon, icosagon and ellipse were analysed (*Figure 2)*. The polygons listed were analysed to obtain the effect of the numbers of polygon side to the pole displacement.

Aluminium alloy 2014 was selected as the pole material in the analysis. The material was defined based on the most commonly used material by current pole manufacturer as discussed in the introduction. Idealisation technique in Pro-Mechanica was used to simplify the model for analysis. Idealisation is a technique of simplifying a model structure for easy and fast analysis.

The six cross-section shapes were tested in five conditions:

1. Test 1 – Unloaded and middle constrained pole for each cross-section with same circumradius (circumradius is a radius of circle circumscribed around a polygon)
2. Test 2 – Unloaded and one end constrained pole for each cross-section with same circumradius
3. Test 3 – Unloaded and middle constrained pole for each cross-section with same weight
4. Test 4 – Unloaded and one end constrained pole for each cross-section with same weight
5. Test 5 – Loaded and one end constrained pole for each cross-section with same weight

In Test 1 and Test 2, the circumradius and thickness for each cross-section shape were standardised to 20 mm and 1.4 mm respectively, similar to the common pole size in the market (Abdul Razak 1999). The pole weight for each cross-section was calculated by using the formulas below:

$$\text{Weight} = \text{Material density } (p) \times \text{volume } (v) \quad \text{eq. 1}$$

Where volume is,

$$V = \text{Cross-section area } (A) \times \text{length} \quad \text{eq. 2}$$

In order to have equal weight pole for each cross-section shape in Test 3, Test 4 and Test 5, each shape was standardised to equal to the area of circular cross-section of 169.77 mm^2. By using the formulas and equation below, each of cross-section shape circumradius was calculated.

Area of a circular cross-section

$$A = \pi r^2 \quad \text{eq. 3}$$

Area of a circular tube cross-section

$$A_o = \pi (r_o - r_i)^2 \quad \text{eq. 4}$$

Area of a polygon cross-section

$$A_p = \frac{1}{2} N.\sin (\frac{360}{N}). r^2 \quad \text{eq. 5}$$

Where N is the number of polygon side

Area of a polygon tube cross-section

$$A_{po} = \frac{1}{2} N.\sin (\frac{360}{N}). (ro - ri)^2 \quad \text{eq. 6}$$

Where (inner circumradius) with given thickness of the polygon is

$$r_i = r_o - \frac{t}{\cos(\frac{360}{2N})} \quad \text{eq. 7}$$

Area of an ellipse cross section

$$A_e = \pi.r_A.r_B \quad \text{eq. 8}$$

Area of an ellipse tube cross section

$$A_e = \pi.(r_A.r_B - r_a.r_b) \quad \text{eq. 9}$$

The thickness of cross-sections in Test 3, Test 4 and Test 5 were standardised to 1.4 mm as in Test 1 and Test 2.

There were two conditions of constrains applied for the analysis model, middle as in *Figure 3* and one end constrains as in *Figure 4* and *Figure 5*. Middle constrained pole is to illustrate a pole that is carried on the shoulder during transportation and one end constrained pole is used for harvesting. For loaded pole, it is to illustrate a cutting device mounted at the one end of the pole. Load of 1.5 kg was used as an average weight of cutting device (Abdul Razak 2002).

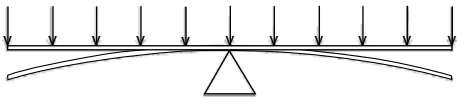

Figure 3. Unloaded middle contrained pole

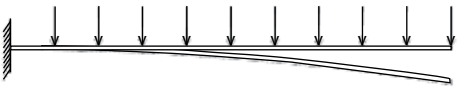

Figure 4. Unloaded one end constrained pole

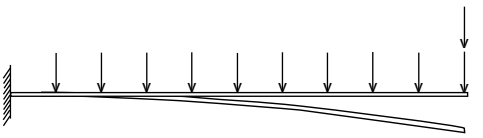

Figure 5. Loaded one end constrained pole

Pro-Mechanica static analysis was selected to obtain the result of the displacement. Multi-pass adaptive was selected as a convergence method with limits of 25%. Convergence is a method to find an optimal mesh to get a better result.

The results obtained from the analyses were analysed using Analysis of Variances (ANOVA) without replication. Significant difference among means were based on a 0.05 by an overall rating method (Atila 1996).

Results and discussion

The calculated area, volume and weight of each cross-section shape of the pole for same tube thickness and circumradius are shown in *Table 1*. A circular cross-section is the heaviest (4.27 kg), while pole with ellipse cross-section is the lightest (4.02 kg). The difference of weight is influenced by the cross-section shape, where the area of a circular cross-section is the highest (169.772 mm^2) and an ellipse cross-section is the lowest (159.879 mm^2).

Table 2 shows the calculated circumradius of the different cross-section shape for the equal pole weight. The calculated circumradius was based on circular cross-section area (169.772 mm^2) with same thickness as before (1.4 mm). Most of the calculated circumradius of the polygon shapes and ellipse were higher than the circumradius of the circular shape. The equal weight was achieved by having the same volume of the material used for the poles. By using equation 7, an equal weight of 4.27 kg was obtained.

Table 1. Calculated area, volume and weight of pole by different cross-section shape

Cross-section shape	Area (mm^2)	Volume (mm^3)	Weight (kg)
Circular	169.772	1527948	4.27
Ellipse	159.876	1438884	4.07
Hexagon	161.210	1450890	4.05
Octagon	164.947	1484523	4.15
Decagon	166.681	1500129	4.19
Icosagon	168.998	1520982	4.25

Table 2. Calculated circumradius of different cross-section shape for equal weight of pole

Cross-section shape	Number of side	Circumradius
Circular	1	20
Hexagon	6	21.02
Octagon	8	20.56
Decagon	12	20.36
Icosagon	20	20.02
Ellipse	1	21.335 max, 18.66 min

Tables 3 and *4* show the results of the analysis for each pole's cross-section that has the same circumradius. The difference between Test 1 and Test 2 was the applied constrains, where one was at the middle and the other at the end of the pole respectively. Both tables show the highest value of the maximum displacement occurred to the pole with ellipse cross-section (128.0302 mm and 2048.3379 mm respectively) and the lowest with the circular cross-section (103.0477 mm and 1552.4421 mm respectively). Both results show the cross-section shapes significantly (p <0.05) affected the pole displacements.

Tables 5, 6 and *7* are the analysis results of each different cross-section with an equal pole weight. These tests were conducted to eliminate the pole body weight effect. The cross-section shape of a pole has significant (p <0.05) effect to the displacement. An ellipse cross-section in vertical orientation shows the lowest displacement for all of the three results obtained (93.3773 mm, –1493.8923 mm and –2893.8389 respectively).

Table 8 shows all the testing results of the pole maximum displacement for each cross-section. The results show the displacement is significantly (p <0.05) affected by the cross-section shape. The difference in displacement occurred due to second moment of inertia of the cross-section area. Second moment of inertia is related to the shape and orientation of the cross-section (Hibbler 2008). Effect of orientation to the second moment of inertia was proven by the result of ellipse cross-section analysis. Vertical and horizontal orientation of the ellipse cross-section had different displacement value for all tests. *Table 9* shows the value of second moment of inertia for each cross-section for the equal pole weight. The value was obtained from Pro-Mechanica analysis software.

An ellipse cross-section in vertical orientation has highest value of second moment of inertia and ellipse cross-section in horizontal orientation is the lowest. Although the shape and size are the same, the values are different due to the different maximum perpendicular distance to the rotating axis. For more detail, refer to the illustration in *Figure 6*, where $a \neq b$

A number of sides of a polygon significantly affected (p <0.05) the pole displacement (*Table 10*). Increasing the number of polygon sides will reduce the maximum value of pole displacement as shown in *Figure 7*. More number of sides will close the polygon to a circular shape.

Table 11 shows the overall rating of final evaluation of the candidate cross-sections for harvesting pole. Each design requirement and factor was weighted depending on the important level which was referred as 'a', 'b', 'c' and 'd' in overall rating(G) equation which are valued to 5, 3, 5, and 4 respectively. From the calculated G value, circular and icosagon cross-section gave the highest rating (6.9%) followed by decagon (5.6%), octagon (5.1%), ellipse (4.2%) and hexagon (2.3%). This shows that the best among the shapes are circular and icosagon. The overall rating gave a small percentage due to small differences

Table 3. Displacement of unloaded and middle constrained pole for each different cross-section with the same circumradius and thickness (Test 1)

Pole length (mm)	Displacement (mm)						
	Circular	Hexagon	Octagon	Decagon	Icosagon	Ellipse	Ellipse vertical
0	–103.0477	–124.9879	–114.8460	–110.4413	–104.8405	–128.0302	–106.3221
1125	–68.8378	–83.4913	–76.7168	–73.7746	–70.0335	–85.5234	–71.0231
2250	–36.5036	–44.2714	–40.6794	–39.1194	–37.1358	–45.3488	–37.6605
3375	–10.8746	–13.1863	–12.1167	–11.6521	–11.0614	–13.5072	–11.2177
4500	0.0000	0.0000	0.0000	0.0000	0.0000	0.0000	0.0000
5625	–10.8746	–13.1863	–12.1167	–11.6521	–11.0614	–13.5072	–11.2177
6750	–36.5036	–44.2714	–40.6794	–39.1194	–37.1358	–45.3488	–37.6605
7875	–68.8378	–83.4913	–76.7168	–73.7746	–70.0335	–85.5234	–71.0231
9000	–103.0477	–124.9879	–114.8460	–110.4413	–104.8405	–128.0302	–106.3221

Negative (–) sign refers to downward direction

Table 4. Displacement of unloaded and one end constrained pole for each different cross-section with the same circumradius and thickness (Test 2)

Pole length (mm)	Displacement (mm)						
	Circular	Hexagon	Octagon	Decagon	Icosagon	Ellipse	Ellipse vertical
0	0.0000	0.0000	0.0000	0.0000	0.0000	0.0000	0.0000
2250	–163.7580	–237.5978	–187.8452	–178.7617	–167.3696	–216.0517	–179.4193
4500	–549.8517	–797.8198	–630.7551	–600.2527	–561.9984	–725.4722	–602.4596
6750	–1037.0022	–1504.6852	–1189.6001	–1132.0721	–1059.9236	–1368.2388	–1136.2334
9000	–1552.4421	–2252.6057	–1780.9030	–1694.7793	–1586.7678	–2048.3379	–1701.0082

Negative (–) sign refers to downward direction

Table 5. Displacement of unloaded and middle constrained pole for each different cross-section with the same weight (Test 3)

Pole length (mm)	Displacement (mm)						
	Circular	Hexagon	Octagon	Decagon	Icosagon	Ellipse	Ellipse vertical
0	–103.0477	–112.7245	–108.4220	–106.4630	–103.8873	–114.9353	–93.3773
1125	–68.8378	–75.2997	–72.4257	–71.1172	–69.3967	–76.7764	–62.3764
2250	–36.5036	–39.9281	–38.4042	–37.7104	–36.7982	–40.7110	–33.0759
3375	–10.8746	–11.8929	–11.4391	–11.2325	–10.9609	–12.1261	–9.8524
4500	0.0000	0.0000	0.0000	0.0000	0.0000	0.0000	0.0000
5625	–10.8746	–11.8929	–11.4391	–11.2325	–10.9609	–12.1261	–9.8524
6750	–36.5036	–39.9281	–38.4042	–37.7104	–36.7982	–40.7110	–33.0759
7875	–68.8378	–75.2997	–72.4257	–71.1172	–69.3967	–76.7764	–62.3764
9000	–103.0477	–112.7245	–108.4220	–106.4630	–103.8873	–114.9353	–93.3773

Negative (–) sign refers to downward direction

Table 6. Displacement of unloaded and one end constrained pole for each different cross-section with the same weight (Test 4)

Pole length (mm)	Displacement (mm)						
	Circular	Hexagon	Octagon	Decagon	Icosagon	Ellipse	Ellipse vertical
0	0.0000	0.0000	0.0000	0.0000	0.0000	0.0000	0.0000
2250	–173.8941	–190.2233	–182.9628	–179.6570	–175.3106	–193.9540	–157.5750
4500	–583.8858	–638.7399	–614.3588	–603.2578	–588.6624	–651.2676	–529.1060
6750	–1101.1895	–1204.6591	–1158.6755	–1137.7389	–1110.2115	–1228.2867	–997.8864
9000	–1648.5334	–1803.4467	–1734.6058	–1703.2621	–1662.0515	–1838.8190	–1493.8923

Negative (–) sign refers to downward direction

Table 7. Displacement of loaded and one end constrained pole for each different cross-section with the same weight (Test 5)

Pole length (mm)	Displacement (mm)						
	Circular	Hexagon	Octagon	Decagon	Icosagon	Ellipse	Ellipse vertical
0	0.0000	0.0000	0.0000	0.0000	0.0000	0.0000	0.0000
2250	–306.6641	–335.4664	322.6619	–316.8318	–309.1666	–342.0458	–277.8885
4500	–1066.6638	–1166.8826	–1122.3414	–1102.0615	–1075.3976	–1189.7692	–966.5957
6750	–2078.8008	–2274.1392	–2187.3315	–2147.8074	–2095.8413	–2318.7434	–1883.7941
9000	–3193.3909	–3493.4829	–3360.1301	–3299.4133	–3219.5835	–3562.0037	–2893.8389

Negative (–) sign refers to downward direction

Table 8. Maximum displacement for each testing by different pole cross-section shape and analysis of variance for the significant difference of each test

Test	Circular	Hexagon	Octagon	Decagon	Icosagon	Ellipse	P value
Test 1	103.0477	124.9879	114.8460	110.4413	104.8405	128.0302	0.000
Test 2	1552.4421	2252.6057	1780.9030	1694.7793	1586.7678	2048.3379	0.001
Test 3	103.0477	112.7245	108.4220	106.4630	103.8873	114.9353	0.000
Test 4	1648.5334	1803.4467	1734.6058	1703.2621	1662.0515	1838.8190	0.001
Test 5	3193.3909	3493.4829	3360.1301	3299.4133	3219.5835	3562.0037	0.002

There was significant difference within shape based on $p < 0.05$

Table 9. Maximum displacement for each testing by different pole cross-section shape and analysis of variance for the significant difference of each test

Test	Hexagon	Octagon	Decagon	Icosagon	P value
Test 1	124.9879	114.8460	110.4413	104.8405	0.000
Test 2	2252.6057	1780.9030	1694.7793	1586.7678	0.014
Test 3	112.7245	108.4220	106.4630	103.8873	0.000
Test 4	1803.4467	1734.6058	1703.2621	1662.0515	0.014
Test 5	3493.4829	3360.1301	3299.4133	3219.5835	0.017

There was significant difference within shape based on p <0.05

Table 10. Value of second moment of inertia for each pole cross-section with an equal weight

Cross-section shape	Circular	Hexagon	Octagon	Decagon	Icosagon	Ellipse	Ellipse (vertical)
Moment inertia (mm^4)	31660.7	28940.6	30089.1	30642.9	314027	28391.9	3944.3

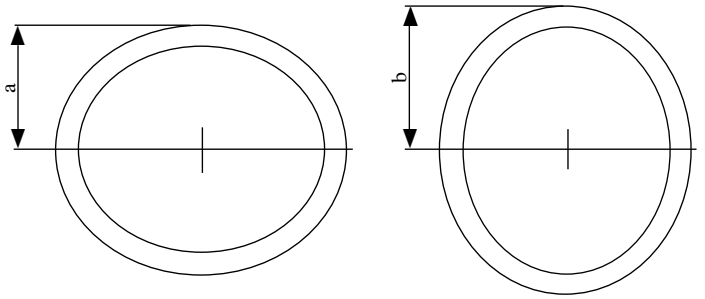

Figure 6. Illustration of ellipse cross-section in horizontal and vertical orientation

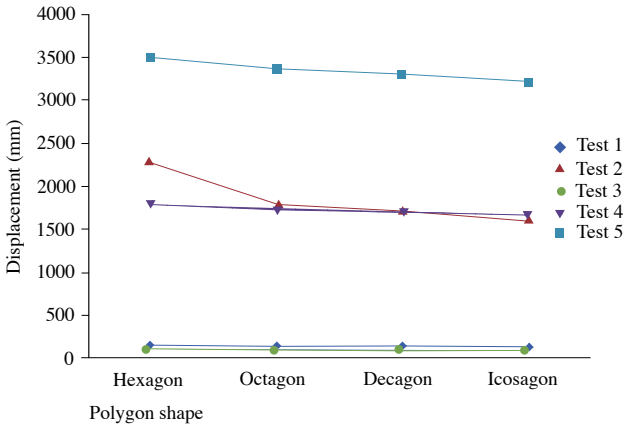

Figure 7. Displacement of polygonal cross-section pole by difference of number of a polygon side

Table 11. Final evaluation of the candidate cross-section shapes for harvesting pole

Cross-section candidates	Weight(a)		Maximum displacement without load (b)		Maximum Displacement with load (c)		Maximum displacement for different orientation (d)		Overall Rating (G)
	A_1	R_1	A_2	R_2	A_3	R_4	A_5	R_5	$\frac{a(1-R_1)+b(1-R_2)+c(1-R_3)+d(1-R_4)}{a+b+c+d}$
Circle	4.27	1.00	1648.53	0.90	3193.39	0.90	103.0477	0.91	0.069 / 6.9%
Hexagon	4.07	0.95	1803.45	0.98	3493.48	0.98	112.7245	1.00	0.023 / 2.3%
Octagon	4.05	0.95	1734.61	0.94	3360.13	0.94	108.422	0.96	0.051 / 5.1%
Decagon	4.15	0.97	1703.26	0.93	3299.41	0.93	106.463	0.94	0.056 / 5.6%
Icosagon	4.19	0.98	1662.05	0.90	3219.58	0.90	103.8873	0.92	0.069 / 6.9%
Ellipse	4.25	1.00	1838.82	1.00	3562	1.00	93.37735	0.83	0.042 / 4.2 %

between the highest and lowest value that were used for calculating the ration value 'R' in *Table 11*. All the design requirement and factor were taken for minimum value for consideration; means better shape should have minimum weight and displacement.

Conclusion

Cross-section shapes are important attributes to be considered in designing harvesting pole. Cross-section shape affected the weight, deflection and also the handling of the pole. Fixed circumradius of a cross-section may affect the pole weight for different cross-section while fixed weight will affect the size. Although the loads applied (weight) to the pole size were the same, there were differences in displacement due to the value of second moment of inertia. This study showed that circular and icosagon shapes were the best shape for a harvesting pole.

References

Abd. Halim, H. (1988). An improved FFB harvesting pole – With special reference to PORIM aluminium harvesting pole. Paper presented at the National Oil Palm Conference, 11 – 15 Oct. 1988, Kuala Lumpur. Organiser: PORIM

Abdul Razak, J. (1999). Harvesting Pole (Zirafah), PORIM Information Series, PORIM TT No.2 October 1999, ISSN 0128 – 5726

—— (2002). Design and evalutation of an improved aluminium harvesting pole (Hi-Reach) for tall palm harvesting. *Oil Palm* 44: 29 – 38

—— (2008). Cantas – A tool for the efficient harvesting of oil palm fresh fruit bunches. *Journal of Oil Palm Research* 20: 548 – 558

Atila, E. and Jesse C. Jones. (1993) Design analyses for material selection. In: *The Engineering Design Process*, (Clif, R, ed.) p. 132 – 188. Texas: John Wiley & Son, Inc.

Hibbler, R.C. (2008). Bending. In: *Mechanics of materials*, 7th Edition, (Fan, S.C., ed.), p. 271 – 371. Nanyang: Pearson Education South Asia Pte. Ltd.

Malek, M. (1993). Economic of mechanisation in oil palm cultivation in Malaysia. Paper presented to the Technical Advisory Communitee, 6 – 7 Dec. 1993, Kuala Lumpur Organiser: PORIM

Suvo (2010). Steps required to perform a finite element analysis. Retrieved on 28 June 2012 from http://www.brighthub.com/engineering/mechanical/articles/66732.aspx#

Abstrak

Galah adalah satu keperluan utama dalam aktiviti penuaian yang melibatkan pokok tinggi. Sebatang tiang yang panjang sentiasa menghadapi masalah lenturan dan berat. Kajian mengenai bentuk keratan rentas tiang penuaian boleh memberi maklumat mengenai reka bentuk yang terbaik. Ujian makmal memerlukan kos yang tinggi dan masa yang panjang untuk dilakukan. Analisis unsur terhingga yang menggunakan perisian komputer adalah cara yang terbaik dan murah. Enam reka bentuk keratan rentas galah telah diuji untuk mendapatkan lenturan dengan menggunakan perisian Pro-Mechanica. Enam bentuk yang diuji tersebut adalah bulat, heksagon, oktagon, decagon, icosagon dan elips. Lima ujian yang terdiri daripada gabungan tiga keadaan tiang, berbeban/tanpa beban, kekangan akhir/hujung dan keberatan sama/berbeza dilaksanakan. Keputusan analisis menunjukkan bahawa bentuk keratan rentas bulat adalah bentuk yang kuat untuk menahan lenturan. Keratan rentas bentuk elips mempunyai lenturan nilai yang berbeza bergantung pada orientasi. Penilaian akhir menunjukkan bulat dan icosagon adalah keratan rentas yang terbaik untuk galah penuaian.